

A Preliminary Investigation of Semi-active Roll Control

Edwin Stone and David Cebon
Cambridge University Engineering Department

Trumpington Street
Cambridge
CB2 1PZ
Phone: 01223 766320
Fax: 01223 332662
Email: ejs43@cam.ac.uk

The roll/ride trade off is a fundamental challenge to vehicle dynamicists. One solution is the use of active suspensions. The weight, cost and power consumption are the main disadvantages of such systems. A semi-active roll control system addresses these issues to some extent. This paper investigates the potential performance gains of such a system through a simple roll plane model. It is concluded that significant improvements in both ride and roll performance are possible. It is found that rate of lateral acceleration rise is a key parameter in the design of a roll controller.

Keywords/ Control, Heavy, Ride, Roll, Roll-over, Semi-active, Vehicle

1 INTRODUCTION

The roll/ride trade-off of suspension systems has been a long-standing challenge for vehicle dynamicists. Achieving better ride performance almost invariably leads to increased roll of the vehicle. To the car engineer this roll leads to undesirable handling characteristics. To the heavy vehicle engineer the increased roll leads to higher risk of roll-over due to the translation of the center of gravity (CoG) of the vehicle.

The problems with heavy vehicle roll-overs have been well documented, for example [1,2]. Roll-overs occur when the overturning moment on the vehicle, due to lateral acceleration and displacement of CoG, exceed the restoring forces that the tyres can supply. A static balance is no longer possible and the CoG must accelerate outwards. Statistics indicate that the less stable the vehicle, the more likely it will be involved in a roll-over accident [3]. This indicates that it is difficult for a driver to anticipate the roll-over limit of the vehicle. Studies have shown that avoidance of roll-over can only be achieved in most cases by improving the stability of the vehicle [1,4].

Design of conventional passive suspensions inevitably involves a compromise between the ride and roll performance. The final choice is likely to depend on the intended operation of the vehicle.

By using active suspension systems, it is possible to gain improvements in both roll and ride performance simultaneously, reducing the need to trade one against the other. A number of different types of active suspensions have been investigated by researchers in recent years. Very few have been adopted by manufacturers of production vehicles. Much of this is to do with the increased cost, complexity, power consumption and weight such systems tend to bring with them.

A semi-active roll control system of the type considered in this paper would provide the vehicle with a switchable roll stiffness. The low roll stiffness setting would be used when lateral forces on the vehicle are small. This would facilitate good ride performance. The vehicle would switch to the higher roll stiffness configuration when large lateral forces are present. By changing only the roll stiffness of the vehicle, the vertical bounce stiffness is unaffected under all conditions, hence the ride is only modified in response to roll-plane roughness. Such a system could be implemented with minimal power consumption. The increase in weight could be low with careful design. The justification of the cost would depend on the achievable performance gain.

The model described in this paper is based on an articulated vehicle built by the Cambridge Vehicle Dynamics Consortium (CVDC). The trailer has independent air suspensions, with left and right wheel stations connected by anti-roll bars. The anti-roll bars are connected to each trailing arm of the suspension with rubber bushes, and to the body of the vehicle with hydraulic actuators, see Figure 1. These actuators are able to provide energy to the system in active mode, or the system can be used in a semi-active configuration. In this configuration the actuators can be set to be rigid which connects the anti-roll bar to the vehicle body, providing a high level of roll stiffness. This mode shall be referred to as the anti-roll bar being "locked". The actuators may also be set so that they are essentially free, and transmit little force. This effectively decouples the anti-roll bar from the system and provides a low roll stiffness configuration. This shall be referred to as the anti-roll bar being "unlocked".

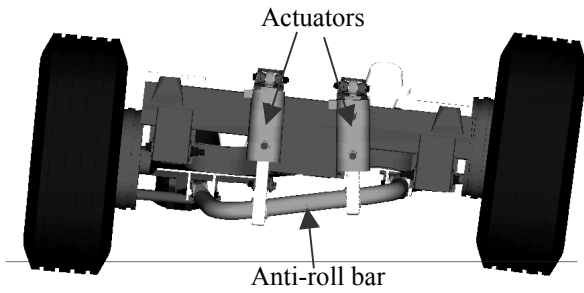


Figure 1 – CAD drawing of active suspension

2 ANALYSIS OF RIDE

A half car roll plane model was used to investigate the ride performance of the vehicle while travelling over an “isotropic” road surface [6]. Left and right wheels received correlated but unequal inputs. The difference in ride performance with and without the anti-roll bar was of particular interest.

2.1 Construction of model

A diagram of the roll plane ride model is included in Figure 2. It is a similar model to that used by Cole [5]. The model has five degrees of freedom: vehicle roll, anti-roll bar roll, body vertical displacement, left and right wheel vertical displacements. The model is of an independent type suspension. In the absence of an anti-roll bar, such a suspension exhibits low roll stiffness: provided entirely by the suspension springs. The more common trailing arm suspensions with rigid axles, used in heavy trailers possess a much higher inherent roll stiffness.

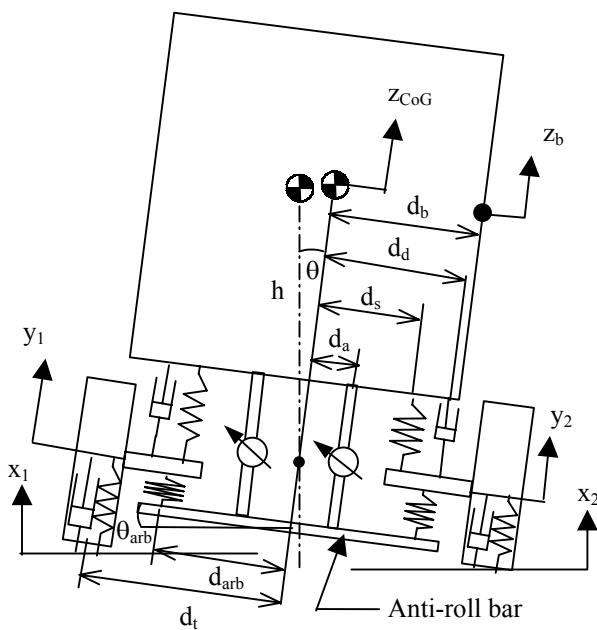


Figure 2 – roll plane model of semi-active independent trailing arm suspension

With the anti roll-bar unlocked, the anti-roll bar provides no restoring moment hence θ_{arb} does not enter the equations of motion. If the anti-roll bar is locked, $\theta_{arb}=\theta$. This reduces the number of degrees of freedom of the system to four. Differential movement of the wheels relative to the body lead to a moment on the

body. This may be provided by the wheels being at different heights and the body being level (single wheel input) or the wheels being at equal heights and the body at an angle (body roll).

By considering the model it is possible to generate four equations of motion. These equations can be solved in the time domain or linearised and solved in the frequency domain.

From both methods of simulation the root mean square (RMS) body accelerations and RMS tyre forces can be calculated and used to compare the ride quality.

2.2 Time response

To solve the equations in the time domain, it is most convenient to rearrange them into state space form. This provides eight first order differential equations which can be solved by numerical integration. The model was non-linear due to the modeling of wheel hop, although none is seen in the results shown here.

2.3 Correlated road profile

The road profile was simulated by first taking a spectral density of the form suggested by Robson [6] for a “good” road. The method used to convert this to two correlated road profiles was that described by Cebon [7]. Correlation between the profiles at large wavelengths is high, whilst correlation at shorter wavelengths is low. The profiles contained 4096 points at 0.1m spacing.

2.4 Random road input

The vehicle was simulated travelling along the random road at 80km/h. Figure 3 shows the simulated body roll angle, both in the anti-roll bar locked case and anti-roll bar unlocked case. With the anti-roll bar unlocked the excursions of roll angle are smaller in magnitude and lower in frequency than in the locked case demonstrating better isolation of the body from the road input.

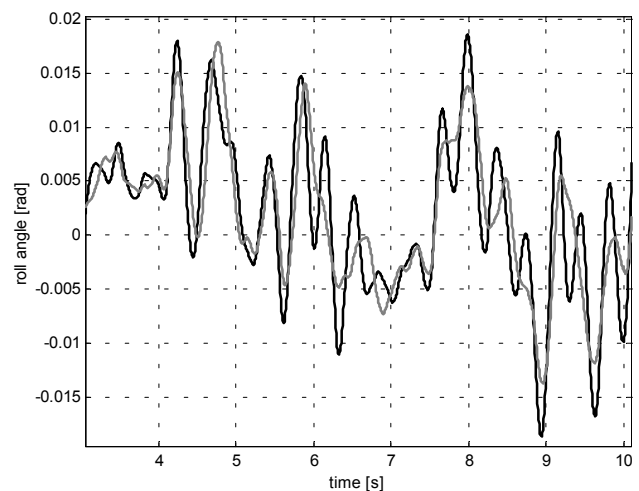
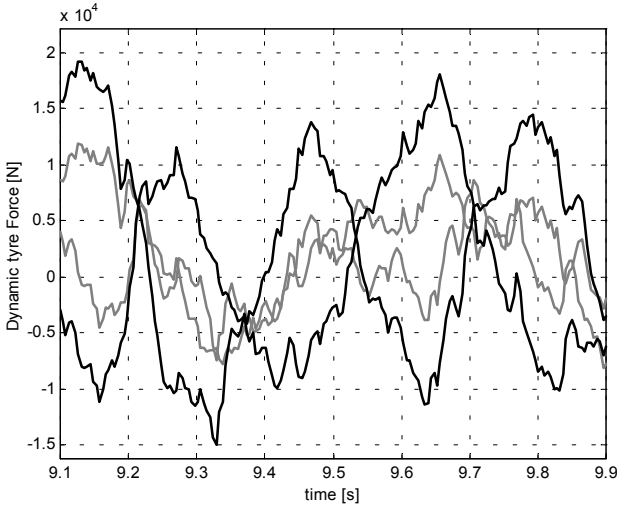


Figure 3 – simulated body roll angle time history for a “good” isotropic road surface at 80km/h
locked (—) unlocked (---)

Figure 4 shows dynamic tyre force time histories. Locking the anti-roll bar increases the tyre forces. Data from the locked case forms an envelope around the unlocked data. It should be noted that the tyre force is

the dynamic component, the static component having been removed.



**Figure 4 – simulated dynamic tyre force time history for a “good” isotropic road surface at 80km/h
locked (—) unlocked (---)**

Figure 5 shows the “body acceleration”, which is the vertical acceleration “measured” at edge of the body, labeled z_b on Figure 2. This is the maximum vertical acceleration on the body and is calculated as:

$$\ddot{z}_b = \ddot{z}_{CoG} + \dot{\theta}d_b \quad (1)$$

With the anti-roll bar locked, the accelerations are larger in magnitude and of higher frequency than with the anti-roll bar unlocked. The extra magnitude is entirely down to the θ component. The vertical acceleration of the CoG is unchanged by the introduction of the anti-roll bar (since the anti-roll bar does not influence the bounce mode of the vehicle).

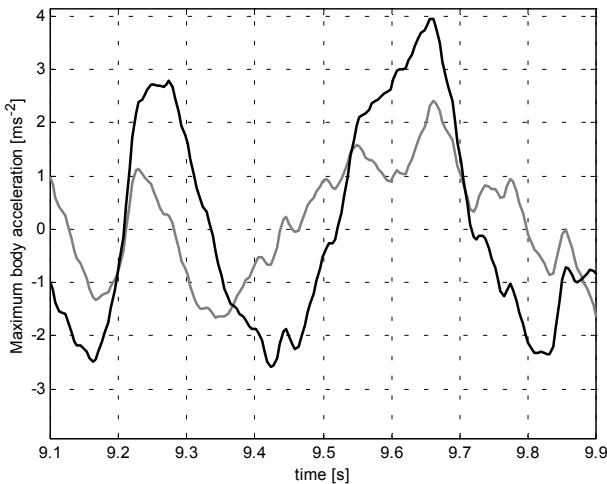


**Figure 5 – simulated maximum body acceleration time history for a “good” isotropic road surface at 80km/h
locked (—) unlocked (---)**

2.5 Frequency domain analysis

Whilst the time domain analysis provides an insight into the behavior of the vehicle that is intuitively

easy to understand, further information can be gained by analysing the vehicle in the frequency domain.

2.6 Transfer function from frequency analysis

Figure 6 shows the tyre force spectral density in response to a vehicle driving at 80km/h over a “good” road. The spectral density with the anti-roll bar locked exhibits a small peak at just under 2Hz due to body bounce and a much larger, but narrower peak at just under 3Hz due to body roll. Also calculated is the Dynamic Load Coefficient (DLC):

$$DLC = \frac{RMS \text{ dynamic tyre force}}{\text{static tyre force}} \quad (2)$$

This was obtained by integrating the spectral density using the method described in [7]. With the anti-roll bar locked, $DLC = 0.20$.

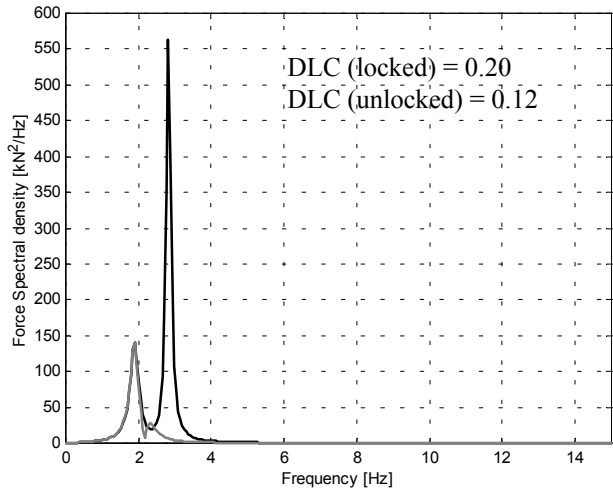


**Figure 6 – simulated tyre force spectral density for a “good” isotropic road surface at 80km/h
locked (—) unlocked (---)**

The spectral density for the case when the anti-roll bar was unlocked is also shown in Figure 6. This has the same body bounce peak at just under 2Hz as the locked case. However, the body roll peak is much smaller in magnitude and also shifted to a lower frequency, mirroring the behavior in the time domain simulation in Figure 4. In this case the DLC is 0.12, a reduction of 40%.

There is also a small magnitude wheel hop peak at around 11Hz, but it is not visible in Figure 6 due to the scale.

The body acceleration spectral density is shown in Figure 7 (see definition of body acceleration in section 2.4). This shows the same behavior as the dynamic tyre force spectral density. The RMS body acceleration with the anti-roll bar locked is $\sigma_{BA}(\text{locked}) = 2.46\text{ms}^{-2}$ while $\sigma_{BA}(\text{unlocked}) = 1.36\text{ms}^{-2}$, a reduction of 45%.

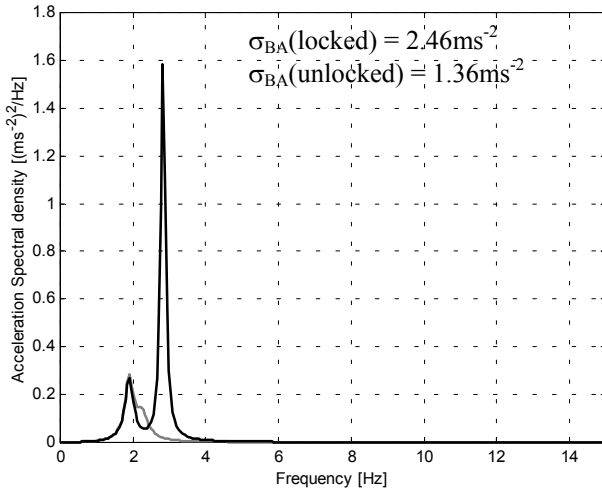


Figure 7 – simulated body acceleration spectral density for a “good” isotropic road surface at 80km/h
locked (—) unlocked (---)

3 ANALYSIS OF ROLL

The half car roll model was used to once again capture the roll behavior of the vehicle. This time lateral acceleration was used as the input to the model to simulate the vehicle performing a change of direction. The normalised lateral load transfer, Δf , that resulted from the lateral acceleration was the key performance parameter:

$$\Delta f = (F_1 - F_2) / (F_1 + F_2) \quad (3)$$

where F_1 and F_2 are the vertical loads on the left and right wheels. When $\Delta f = 0$, the loads on the wheels are equal. Wheel lift occurs at $\Delta f = \pm 1$, the sign being determined by which wheel is lifting. Wheel lift in a real, multi-axle, vehicle does not necessarily mean roll-over [1]. However, this paper shall take wheel lift as the threshold at which stability is evaluated. The difference in performance of the vehicle, with and without an anti-roll bar, was considered. Furthermore, the performance based on the anti-roll bar being locked at some threshold value of lateral acceleration after the manoeuvre had commenced was considered.

3.1 Construction of model

The model was broadly similar to that shown in Figure 2 but differed in the following respects. The road surface was no longer an input and was modeled as a rigid plane. The input was provided by lateral acceleration acting at the center of gravity. To simulate the effect of switching the anti-roll bar from one condition to another during the simulation, a model of the component connecting the anti-roll bar to the body was required. This was modeled as shown in Figure 8 and represents the hydraulic cylinders on the CVDC vehicle which are used to control the anti-roll bars.

The roll model had three degrees of freedom: rotation of the body, rotation of the anti-roll bar, and compression of the oil in the hydraulic cylinder. Three equations describing the dynamics of the system can be written. Transforming into state space form leads to a

five first order differential equations which can be solved by numerical integration.

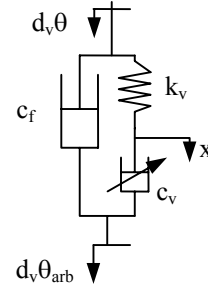


Figure 8 – model of actuator

3.2 Steady state

Steady state behavior of the vehicle was investigated by using a slow ramp input of lateral acceleration. The rate of the ramp was chosen to be much slower than the dynamics of the vehicle so the response represented the vehicle in a quasi steady state condition. The ramp started at zero and increased to 0.6g over 50 seconds.

Initially the vehicle was simulated with the anti-roll bar locked. As the lateral acceleration increases, so does the roll angle in a linear fashion, as shown by the line labeled “locked”, Figure 9. The simulation was repeated with the anti-roll bar unlocked. The roll angle again increases linearly with lateral acceleration but at a faster rate, see the line labeled “unlocked”, Figure 9. The simulation was run again, with the anti-roll bar being initially unlocked and then locked once the lateral acceleration exceeded 0.1g, simulating a simple control system. This was repeated with the threshold, a_{switch} , set at 0.2g, 0.3g and 0.4g. Once the anti-roll bar is locked, the roll angle increases along a line parallel to the “locked” line.

Note that in these simulations, the roll angles reach large values (up to 10 degrees). At these roll angles, a linear model is unlikely to yield accurate results so care must be taken when interpreting the behavior.

The lateral load transfer was calculated and is plotted in Figure 10. With the anti-roll bar locked the vehicle achieves a wheel lift threshold (load transfer = 1) of 0.53g. Unlocking the anti-roll bar reduces this to 0.48g. The higher the threshold at which the anti-roll bar is locked the lower the lateral acceleration at wheel lift. The change is a linear relationship between lateral acceleration at which the anti-roll bar is locked and the lateral acceleration at roll-over.

3.3 Step input of lateral acceleration

A “step input” in lateral acceleration (actually a quarter sine wave) was also applied. The rate of rise was chosen to reflect the rate at which a driver is able to apply steering effort and the way the lateral acceleration then develops in the vehicle as a result of this input and the dynamics of the vehicle.

Firstly, the vehicle was simulated with the anti-roll bar locked. A run was performed and the peak roll angle recorded. The simulation was repeated with the lateral acceleration increased and again the peak roll angle recorded, see Figure 11. This was then repeated for a large number of different lateral accelerations from 0 to 0.5g. Each time the peak roll angle was recorded.

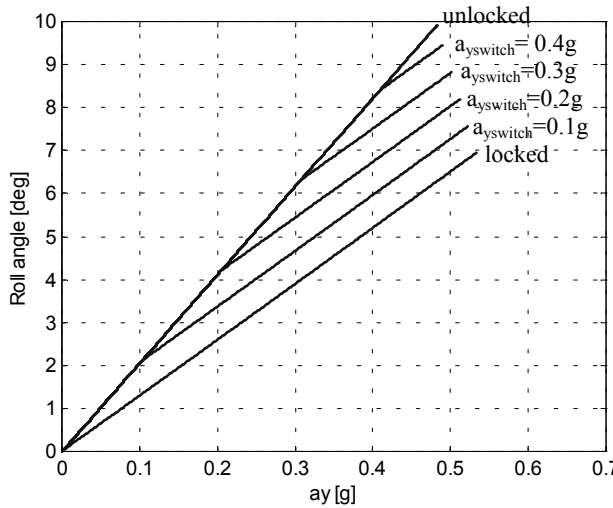


Figure 9 – simulated body roll angle in quasi steady state conditions

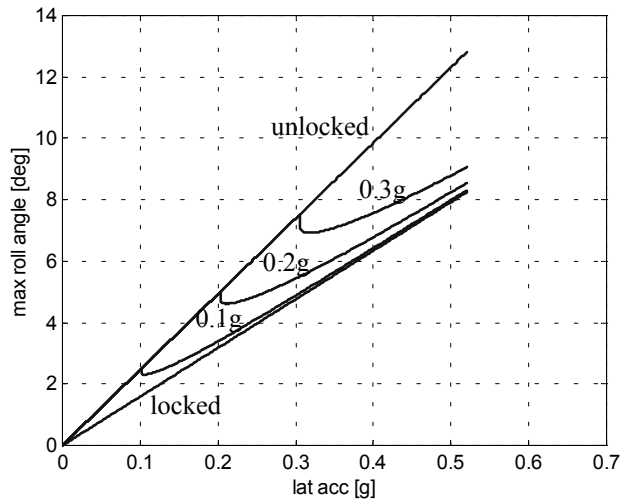


Figure 12 – simulated body roll angle in response to step input

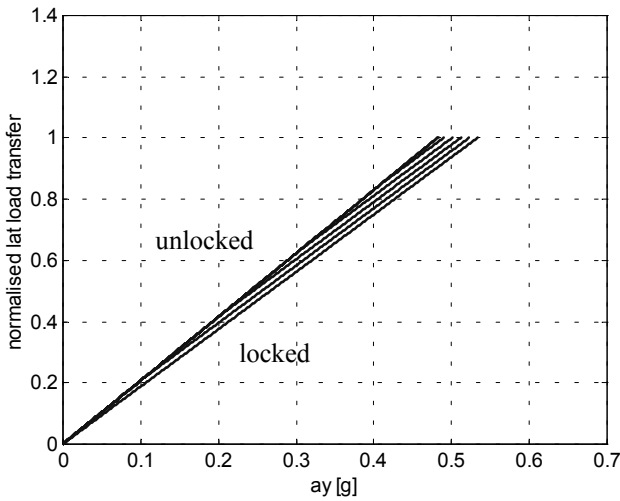


Figure 10 – simulated normalised lateral load transfer in quasi steady state conditions

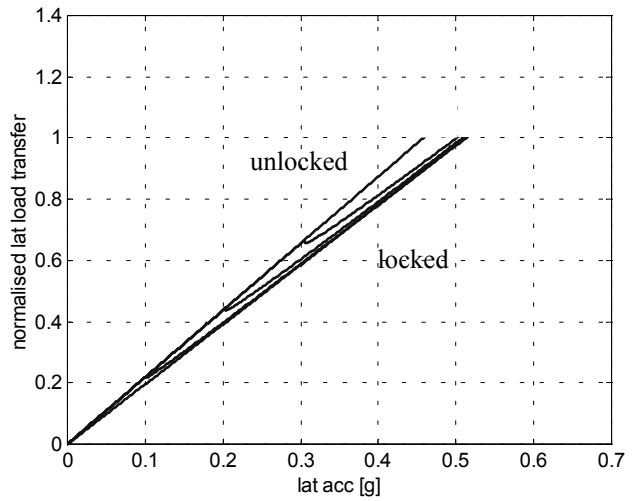


Figure 13 – simulated normalised lateral load transfer in response to step input

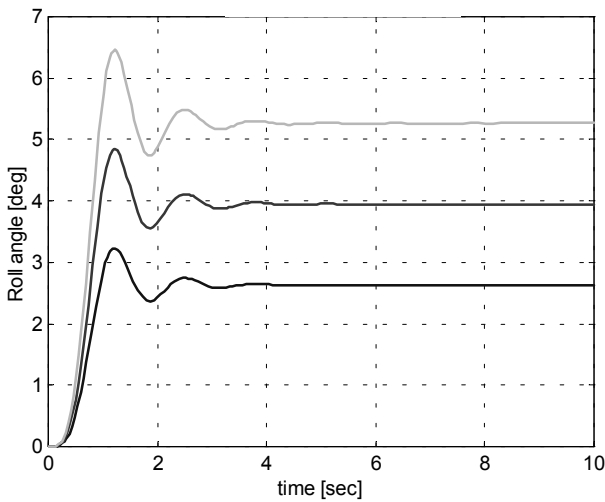


Figure 11 – simulated roll angle time history in response to step input. Each line is the response to a different level of lateral acceleration.

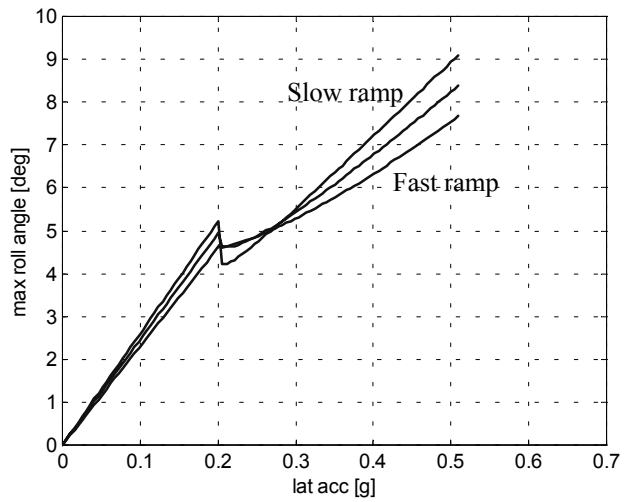


Figure 14 – simulated variation in roll angle response with change in rate of lateral acceleration rise

The peak roll angles are plotted against lateral acceleration for these runs as the line labeled “locked” in Figure 12. The simulations were then repeated with the anti-roll bar unlocked, this generated the line labeled unlocked in Figure 12. A control strategy was then implemented to lock the anti-roll bar when the lateral acceleration exceeded 0.1g. The peak roll angles were once more recorded for a range of lateral accelerations. This was repeated with the control system locking the anti-roll bar at lateral accelerations of 0.2g and 0.3g, see Figure 12. These roll angles are translated into lateral load transfers in Figure 13. For all of these threshold values of lateral acceleration at which the anti-roll bar is locked, the roll-over threshold is close to that of the vehicle in which the anti-roll bar is always locked. They display a considerable improvement over the vehicle which has the anti-roll bar always unlocked.

3.4 Ramp input

To investigate the transition between the rapid rise of the step input and the gradual rise of the steady state simulation, the step input was repeated but with the rate of increase in lateral acceleration reduced. The control system was set to lock the anti-roll bar if the lateral acceleration was greater than 0.2g. As the rate of rise of lateral acceleration is reduced, so the peak roll angle increases in the higher lateral acceleration region of the plot (those at which roll-overs occur), see Figure 14. The explanation is that if the vehicle is rolled out at an angle when the anti-roll bar is locked, the roll angle is “locked in”. The slower rise in lateral acceleration allows the roll angle to build up before the anti-roll bar locks. A large roll angle is then locked in. Rapid increases in lateral acceleration lead to the control system locking the anti-roll bar before the vehicle has had a chance to develop significant roll. Almost zero roll angle is locked in. This has the consequence that the results would look significantly different if a time delay of significant magnitude existed.

4 CONTROL STRATEGY

From the results of the roll analysis, it is clear that the situation where lateral acceleration builds up slowly is very different to that where lateral acceleration increases rapidly. Slow increases in lateral acceleration are likely to be experienced in general driving whilst more rapid rises would be experienced during avoidance manoeuvres. In the latter case, using a lateral acceleration threshold as the control input seems a reasonable strategy as long as the delays in the control system are small. However, in the case where roll angle has a chance to build up due to low rates of increase of lateral acceleration, a more sophisticated control strategy is likely to be beneficial. It may be possible to offset any delays and increase performance by making use of the fact that lateral acceleration is the result of a steering input. By using a steer-speed estimate of lateral acceleration, it is possible to anticipate future values of lateral acceleration by a time approximately equivalent to the wheelbase of the vehicle divided by the vehicle speed. This could be up to 0.65s for a typical heavy vehicle travelling at 80km/h.

5 CONCLUSION

This preliminary analysis into the advantages of a semi-active roll control systems has demonstrated significant benefits in both ride and roll performance. The DLC is reduced by 40% by unlocking the anti-roll bar and the RMS body acceleration is reduced by 45%.

The percentage gains in roll-over threshold are smaller but since work has shown modest increase in rollover threshold leads to a much reduced frequency of roll-overs [1], the 10% increase in roll-over threshold in the “best case” scenario is significant.

The roll analysis further demonstrates that whilst using lateral acceleration as the control input in cases where lateral acceleration rises rapidly, it may be prudent to consider a different controller for situations where lateral acceleration develops more slowly.

6 FURTHER WORK

It is intended to further investigate the effect of the anti-roll bar on the ride of the vehicle, in particular to step inputs. The roll model will be improved to include non-linearities at large roll angles. Also, an investigation is to be made into the design of a controller to cope with both slow and fast increases of lateral acceleration. Experimental testing on the CVDC vehicle to validate both models and control strategy is planned.

7 ACKNOWLEDGEMENTS

The authors would like to acknowledge the support of the following groups for providing funding: EPSRC and the members of the CVDC, consisting of Firestone, Fluid Power Design, General Trailers, Koni Dampers, Mektronika Systems, Meritor HVS, Pirelli, Qinetiq, Shell UK, Tinsley Bridge, Volvo trucks.

REFERENCES

- 1 Sampson, D., “Active Roll control of articulated heavy vehicles”, University of Cambridge. UK, 2000.
- 2 Goldman, R.W., El-Gindy, M. and Kulakowski, B.T., “Roll over dynamics of road vehicles: Literature survey”, Heavy Vehicle Systems, A Series of the Int. J. of Vehicle Design, Vol. 8, No. 2, pp. 103-141, 2001
- 3 Segal, L., “Course on the Mechanics of Heavy-Duty Trucks and Truck Combination, University of Michigan, 1989
- 4 Palkovics, L., Semsey, A., Gerum, E., “ Roll-Over prevention system for commercial vehicles – additional sensorless function of the electronic brake system”, Vehicle Systems Dynamics, 32, pp. 285-297, 1999
- 5 Cole, D.J., Cebon, D., “Truck suspension design to minimise road damage”, Proc. Instn Mech Engrs, Vol 210, pp95-107, 1996.
- 6 Robson, J.D., “Road surface description and vehicle reponse”, Int. J. of Vehicle Design, 1 (1) pp25-35, 1979.
- 7 Cebon, D., “Handbook of vehicle-road interaction”, Swets and Zeitlinger, 1999.